Corticosteroid resistance is predetermined by early immune response dynamics at acute Graft-versus-Host disease onset

One Sentence Summary (150 characters): Steroid-resistant acute graft versus host disease is set at disease onset as evidenced by specific transcriptomic signature, cell-to-cell crosstalk and trajectories.

Sophie Le Grand[1], Yannick Marie[2], Delphine Bouteiller[2], Émilie Robert[3], Régis Peffault de Latour[3,4], Gérard Socié[1,4], Nicolas Vallet[5]*, David Michonneau[1,4]*

Affiliations:

[1]INSERM UMR 1342, Translational Immunology in Immunotherapy and Hematology, IHU Leukemia Institute Paris Saint Louis, Paris Cité University, F-75010, Paris, France

[2]Genotyping and Sequencing Facility, Paris Brain Institute-ICM, Hôpital de la Pitié-Salpêtrière, CNRS UMR 7225, INSERM U1127, Sorbonne Université UM75, CS21414, Paris, France.

[3]Cryostem Consortium, Technopôle de Château Gombert, Marseille, France

[4]Hematology Transplantation, Saint Louis Hospital, Assistance Publique des Hôpitaux de Paris, 75010 Paris, France

[5]Hematology and Cell Therapy department, University Hospital of Tours, Inserm U1069 N2COx

*co-last authors

Corresponding author:

David Michonneau

Saint Louis hospital, hematology and transplantation

1 avenue Claude Vellefaux

75010 PARIS, FRANCE

david.michonneau@aphp.fr

Abstract

Steroid-resistant acute graft versus host disease (SR-aGVHD) is the leading life-threatening complication following allogeneic hematopoietic stem cell transplantation. Novel therapeutics development is impeded by scares knowledge on biological pathways leading to steroid resistance at time of aGVHD diagnosis. To gain insight into our understanding on circulating immune cell subsets and functions at time of aGVHD, a single cell deep phenotyping and transcriptome analysis was performed on peripheral blood mononuclear cells from patients with aGVHD before steroid treatment or without aGVHD. We aimed at identifying biological patterns associated with steroid resistance at early onset of aGVHD. First, circulating immune cell subsets were associated with increased incidence of aGVHD, but not with steroid sensitivity. Then, pathway analysis and inferred ligand/receptor interactions revealed major functional divergences between steroid-sensitive (SS-) and SR-aGVHD, including enrichment of TNFα activation in SR-GVHD, as well as TNF/TNFR, CCL3, CCL4 and IL18 signaling, and decreased interferon α and γ signaling pathways, suggesting that steroid resistance in an intrinsic property of immune cells before any treatment. To go deeper into the understanding of mechanisms at play during SR-aGVHD, we modeled immune trajectories within $CD8^+$ T cells and evidenced specific direct transition, from an early naive state to a highly activated one. By contrast, SS-aGVHD involved specific gene signatures across multiple intermediate differentiation stages during cell-to-cell transitions. These findings provide evidence that steroid resistance is driven by intrinsic mechanisms already present at the onset of alloimmune response, that may serve as potential new therapeutic targets.

INTRODUCTION

Allogeneic hematopoietic stem cell transplantation (HSCT) is a major treatment for hematological malignancies. Its therapeutic effect is based on alloreactivity of donor T cells against tumor cells. However, donor T cells also react against healthy host cells, which may lead to graft-versus-host disease (GVHD). Acute GVHD (aGVHD) may involve skin, gut, or liver tissue. Its pathophysiology is initiated after tissue damage from high dose alkylating agent and radiation based-conditioning regimens leading to recognition of non-self-major and minor histocompatibility antigens (MHC and mHag(*1*)) and an alloreactive immune response, exacerbated by altered tissue repair mechanisms and microbiome dysbiosis(*2*). Despite first line treatment with prompt corticosteroid initiation(*3*, *4*), more than 40% of patients are steroid resistant (SR-aGVHD)(*5*, *6*). Steroid resistance is defined by a progressive disease after three days of standard dose of corticosteroids, an absence of clinical response after 7 days, an absence of complete remission after two to four weeks, or recurrence while steroids are stopped or tapered. Although ruxolitinib improves symptoms for 60% of SR-GVHD patients(*7*, *8*), their prognosis is very dismal(*3*, *7*, *9*).

While biomarkers were recently developed to improve aGVHD diagnosis and risk stratification(*10*–*14*), response to steroid is still unpredictable and biological mechanisms underlying steroid resistance remains only partly understood, even in the few experimental transplantation models of SR–GVHD described(*15*–*17*). In humans, specific whole gene expression analysis at diagnosis of lower intestinal acute SR-GVHD identified an increased repair-associated gene (amphiregulin and the aryl hydrocarbon receptor) and M2 macrophages pathways(*18*), suggesting that steroid resistance in not restricted to the T cells response as initially suspected. Indeed, neutrophils participate in tissue damage at GVHD onset and triggering, through reactive oxygen species production(*19*) and promote T cell expansion(*20*) and differentiation to Th17 cells(*21*, *22*). As corticosteroids increase neutrophils count and development, it has been hypothesized that corticosteroids may trigger a positive feedback loop between pathogenic T cells and neutrophils in SR-GVHD context(*23*).

Furthermore, neutrophil-predominant noncanonical inflammation pathways were recently identified in gut-SR-GVHD biopsies, notably ubiquitin specific peptidase 17–like family of genes(*24*). While gut microbiota's role has been extensively studied in GVHD, it is not well understood in SR-GVHD. Butyrate, a short-chain-fatty-acid product from *Blautia* bacteria is associated with better long terms outcomes in aGVHD(*25*–*27*), but one study found a negative association between butyrate production and SR-GVHD, due to the ability of butyrate to impair human colonic stem cells from recovering epithelial monolayer(*28*). Other studies identified SR-GVHD biomarkers such as IL-22(*15*), but with controversial potential(*29*, *30*). Most of these studies rely on murine models(*15*–*17*, *23*, *31*), and there is currently no clear overview of immune subsets associated with steroid resistance in human GVHD.

We hypothesize that reshaping of immune system might be initiated early in alloimmune responses, therefore predisposing to corticosteroids resistance. To describe immune subsets and their respective function, cellular indexing of transcriptomes and epitopes sequencing (CITE-Seq) was performed on peripheral blood mononuclear cells (PBMC) samples collected at the onset of aGVHD before first line treatment, or in patient without GVHD at day 100 after HSCT. Whole landscape of circulating immune cells at early onset of aGVHD and its association with GVHD severity was uncovered. Deep analysis of transcriptomic profiles revealed that steroid resistance is an intrinsic property of the immune response, characterized by specific enriched biological pathways, specific cell-to-cell crosstalk through ligand-receptor interactions and a specific immune trajectory involving most immune subsets. Altogether, our results highlight that steroid-resistant GVHD is an early characteristic of allo-immune response before any immunosuppressive treatment and pave the way to more targeted first-line therapy to improve allogeneic HSCT outcomes.

52 # RESULTS

53 **Cohort's characteristics**

54 Samples from 53 patients were retrieved from the prospective CRYOSTEM multicenter
55 collection. PBMC were collected before corticosteroids initiation for patients diagnosed with
56 aGVHD, and at day 100 post allo-HSCT for non-GVHD patients. Hematological malignancies,
57 HSCT procedure, clinical and GVHD characteristics were balanced between groups, except
58 for graft source, delay between sample and transplantation date (**Table S1)**. Among the 21
59 aGVHD patients, 16 (76%) were steroid sensitive (SS-GVHD) and 5 (24%) were steroid
60 refractory (SR-GVHD), with a median delay of 24 days [13-96] and 17 days [11-70] between
61 transplantation and sample, respectively (p=0.3) (**Figure 1A**). For validation and control
62 purposes, 6 samples from healthy blood donor were used. After samples preparation for CITE-
63 seq experiments, sequencing, quality control filtering and data processing acquisition, more
64 than 300,000 single cells were available for immune profiling and transcriptome analysis
65 (**Figure 1B**). Unsupervised clustering resulted in the identification of 40 immune cell subsets
66 (**Figure 1C and S1**), characterized by their surface antigens expression (**Figure 1D**).
67

68 **Immune signature and increased proliferation associate with aGVHD onset but not with**
69 **response to steroids**

70 Compared to non-aGVHD patients, classical monocytes CD73^{+} were significantly enriched in
71 aGVHD patients, whereas NK and B cell subsets were significantly decreased (**Figure 1E**). To
72 encompass the compositional structure of immune subsets frequencies, principal coordinates
73 analysis (PCoA) was used. Four distinct immune clusters were identified, thereafter called
74 immunotypes (**Figure 2A**). aGVHD patient's distribution was significantly different among
75 immunotypes (p=0.001, **Table S2**, **Figure 2B**), as well as the GVHD cumulative incidence
76 (**Figure 2C,** Immunotype 4 GVHD incidence = 72% at day 100, *vs* immunotype 1 = 55%, *vs*
77 immunotype 2 = 38%, *vs* immunotype 4 = 0%, global log-rank p=0.005). GVHD-free and

78 relapse-free survival (GRFS) was significantly associated with immunotypes (p=0.0048,
79 **Figure S2**), however there were no significant differences in non-relapse mortality, cumulative
80 incidence of relapse or of chronic GVHD (**Figure S2**), and no association with aGVHD organ
81 involvement (**Table S2**). Association with other clinical variables is depicted in **Figure S3**.

82 Immunotype 1 and 4 included a large number of patients with aGVHD (**Figure 2B–C**)
83 and were characterized by an overall reduction in immune cell heterogeneity, illustrated with
84 an imbalanced immune subsets representation (**Figure 2D**). Especially, immunotypes 1 and 4
85 presented a high display of classical monocytes $CD11b^{bright}$ (IgM^{+} or IgM^{-}) compared to other
86 immunotypes. Immunotype 2 and 3 were characterized by a balanced distribution across
87 different immune cell populations, and a lower classical monocytes $CD11b^{bright}$ cells
88 representation. Remarkably, immunotype 3 was characterized by an absence of patients with
89 aGVHD, a decrease in classical monocytes $CD11b^{bright}$ and in other monocytes populations,
90 whereas effector T $CD4^{+}$ and $CD8^{+}$ were predominantly increased.

91 To further investigate whether the over-representation may encompass a high cell
92 division rate at time of aGVHD diagnosis, we determined cell cycle phase scoring within each
93 immune cell population. Immune populations were predominantly in S phase (**Figure 3A**),
94 reflecting increase cell proliferation at aGVHD onset.

95 No significant differences among immune cells abundances, immunotypes and
96 cell-cycle scoring was observed with respect to corticosteroid resistance (**Figure 2B**, **Table**
97 **S2, Figure S4 and S5**). In summary, immune cells subset clearly identified patients without
98 GVHD but hardly discriminated SS and SR-GVHD. We thus hypothesized that cell intrinsic
99 biological functions may predispose to SR-GVHD.

100

101 **Steroid resistance is associated with enrichment of TNFα and metabolic pathways at**
102 **aGVHD onset**

103 We first considered the biological pathways enriched at the onset of aGVHD by
104 comparison with patients without GVHD (**Figure S6**). When considering aGVHD as a whole,
105 we observe overactivation of IFNα and γ pathways in all immune cells, and a decrease in
106 TNFα signaling, especially in $CD8^+$ T cells and myeloid cells.

107 To study which biological process may correlate with subsequent SS- or SR-aGVHD,
108 we then performed a second enrichment analysis in patients with SS- or SR-aGVHD.
109 Compared to SS-aGVHD, inflammation pathways were enriched in SR-aGVHD patients within
110 all immune cells, particularly TNFα and hypoxia pathways (**Figure 3B**). STAT5 and MTORC
111 pathways were particularly upregulated in exhausted effector memory $CD4^+$ and $CD8^+$ T cells,
112 in naïve $CD8^+$ T cells and in dendritic immune cells. The IL6/JAK STAT pathway was also
113 highly enriched in naive $CD8^+$ T cells and classical $CD11b^{bright}$ monocytes. Genes associated
114 with metabolism pathways were overexpressed, especially oxidative phosphorylation in naïve
115 $CD4^+$ T cells, double negative T cells and myeloid cells. Conversely, there was a decreased
116 activation of the IFNα and γ responses within all immune subsets, except NK cells.

117

118 **Cell to cell crosstalk during SR-GVHD specifically involves IL1, CCL3, CCL4, TNFα and**
119 **IL18 signaling**

120 To address whether cell biological processes involved in SR-aGVHD may be involved in
121 cell-to-cell interactions leading to early steroid-resistance, we examined intercellular
122 communication using a computational inferring method(*32*). When focusing on $CD8^+$ T cells
123 as receiver, 20 ligands were identified as prioritized ligands, and their expression on sender
124 cells is shown in **Figure 4A**. IL1B, CCL3 and CCL4 ligands were particularly overexpressed in

125 SR-aGVHD condition (**Figure 4B**). Regulatory potential of each ligand with predicted targets
126 genes in shown in **Figure 4C**.

127 Predicted ligands and targets interaction were then analyzed for CD4 regulatory T cells
128 (**Figure S7A**), NK cells (**Figure S7B**), $CD4^+$T cells (**Figure S8A**), and double negative T cells
129 (**Figure S8B**). An overview of all these interactions is depicted as a circus plot (**Figure 4D**)
130 based on biologically confirmed interactions previously designated as *bona fide* interactions
131 (**Figure S9A**). TNF ligands-to-cell signaling appeared to be overexpressed in most sender
132 cells in SR-aGVHD patients, as well as CCL3, CCL4 and IL18 signaling. ADAM17, which is
133 involved in TNF activation(*33*), was overexpressed in all senders and interacted with TNFR,
134 ITGAL and ITGB2 receptors. Interestingly, IFN/IFNR interactions was enhanced across all
135 receivers in SR-aGVHD but absent in SS-aGVHD.

136 Conversely, when comparing patients with aGVHD to those without aGVHD, immune
137 cells crosstalk appeared different to that disclosed in the SS- and SR–aGVHD setting
138 (**Figure S9B**). Consistent with enrichment analysis, TNF/TNF-R interaction was decreased
139 among DN T cells, NK cells and T regulatory lymphocytes. TGFB1/TGFBR interactions, which
140 are considered as being associated with an immunoregulatory role, were significantly
141 increased in patient with no aGVHD compared to aGVHD patients, especially within $CD8^+$ T
142 cells. BTLA/TNFRSF14 interaction is another pathway previously identified in animal models
143 as a regulator of alloimmune response(*34*, *35*), and was overexpressed in patients without
144 GVHD.

145

146 **Specific trajectories were associated with SR-GVHD**

147 As biological processes and cell-to-cell interactions targeting $CD8^+$ T cells were associated
148 with SR-aGVHD, we hypothesized that immune cells subsets from SR-aGVHD and SS-
149 aGVHD patients may exert specific $CD8^+$ T cell trajectories. To address this hypothesis,
150 trajectories within $CD8^+$ T cell were defined on a new cell clustering based on mRNA

151 expression (**Figure S10**). Two trajectories were identified for $CD8^+$ T cell: (i) lineage 1
152 described in **Figure 5A-B** and (ii) lineage 2 described in **Figure S11**.
153 Frequency of cells in lineage 1 slightly increased over pseudotime in SS-aGVHD
154 patients through multiple transition states starting from naïve double positive T cell (cluster 27)
155 to effector memory $CD8^+$ T cell expressing ICOS (cluster 2) **(Figure 5A-B).** By contrast,
156 SR-aGVHD patients were characterized by a direct transition with very few cells in the
157 transition subsets (cluster 15, 9 and 10), most immune subset being grouped in cluster 27 at
158 early pseudotime or in cluster 2 in late pseudotime. The same pattern was observed in the
159 second $CD8^+$ T cell trajectory, with a transition from naïve double positive T cell (cluster 27) to
160 $CD8^+$ TEMRA cells expressing ICOS and PD1 (cluster 25) (**Figure S11A-B**).
161 To highlight different gene expression pattern in SS-aGVHD and SR-aGVHD we first
162 studied individual genes whose expression varied significantly along pseudotime and across
163 transition state (**Figure 5C, S11C, Table S3-S10**). Among the most significant genes involved
164 in transition states, we identified CCL4, CCL5, IFI6, LAG3, and TIGIT (**Table S11 and S12**).
165 SR-aGVHD patients exhibited earlier and higher CCL4 and LAG3 expression in pseudotime
166 (**Figure 5D and S11D**). Consistently with pathway enrichment analysis, IFI6 expression,
167 indicative of IFNα activation, was higher in SS-aGVHD patients, particularly in early-
168 differentiated $CD8^+$ T cells.
169 To study overall biological processes, we used hierarchical clustering to identify
170 modules of correlated gene among the top 500 expressed gene along pseudotime lineages.
171 This approach identified 5 modules of genes involved in cell-to-cell transition (**Figure 5C**).
172 Over-representation analysis (ORA) from Gene Ontology knowledgebase within each cell
173 subset highlighted the main biological pathways involved at each transition state (**Figure 5E**).
174 SR-aGVHD was notably associated with an early enrichment of pathways associated with cell
175 activation and high transcriptional and translational activity in naïve double positive T cell
176 (**Figure S11E**). A detailed analysis of pathways enriched in each module revealed striking

177 differences in the dynamics of T cell activation during SR-GVHD (trajectory 1 in **Figure S12**
178 **and S13,** and trajectory 2 in **Figure S14 and S15**).
179 Overall, these results reveal that even before starting corticosteroids, aGVHD is already
180 characterized by different trajectories and pattern of gene activation between transition states,
181 that can define a specific dynamic of alloimmune response during steroid resistance.
182

183 ## DISCUSSION

184 Despite recent advances in the management of aGVHD, steroid-resistant treatment remains
185 a challenge. This study is the first to describe immune subsets and transcriptional profiles in
186 human at time of aGVHD. Early identification of patients at risk of developing steroid resistance
187 is crucial for rapid and tailored therapeutic intervention. Up to now, a comprehensive
188 understanding of the circulating immune cells mechanisms associated with steroid resistance
189 has not been addressed. Our results highlight that steroid resistance is characterized at the
190 onset of aGVHD, by a specific transcriptomic profile that reveal biological pathways, cell-to-cell
191 interactions and trajectories that differ from steroid sensitive patients.
192 Immunotypes and cell cycle scoring enabled the identification of specific patterns
193 associated with aGVHD compared to non-aGVHD patients. Immunotype 4, characterized by
194 poor immune cell diversity and by classical $CD11^+$ monocytes abundance was associated with
195 worsened aGVHD free survival. This observation is consistent with previous studies identifying
196 monocytes and macrophages as fully parts of the immune response at aGVHD onset (*18*, *36*–
197 *39*).
198 However, cell subsets distribution did not allow to distinguish SS- and SR-aGVHD.
199 When focusing on immune cells functions rather than distinct phenotypes, we found specific
200 patterns associated with SR-GVHD, especially higher TNFα pathway activation. This was
201 strengthened with inferred interaction analyses which revealed an increased TNF/TNFR
202 signaling, notably in $CD8^+$ T cells. Although this *in silico* prediction would need to be confirmed

203 *in vivo*, these results might suggest that early anti-TNF therapies could be beneficial in patients
204 with the corticosteroid resistance profile we described herein. This is supported by a previous
205 clinical phase 2 trial testing a combined therapy of anti-TNF and corticosteroids, with increased
206 response rate (69% vs 33%; $P < 0.001$) without increased infections risk(*40*).

207 Our results suggest that the alloimmune response responsible for GVHD is already
208 different at its initiation in patients who will be steroid-resistant. Overall, the integration of our
209 data shows that steroid resistance could result from the cytokine production profile by myeloid
210 populations, especially monocytes producing CCL3, CCL4, IL1, and IL18, which stimulate the
211 activation of naive $CD8^+$ T cells and induce direct differentiation into effector T cells (**Figure 6**).
212 These results are consistent with published data on the role of myeloid populations(*19*, *20*)
213 and inflammasome activation(*41*) in the initiation of acute GVHD in mice, or of M2 macrophage
214 in the gut of patients with SR-GVHD(*18*). Additionally, previous data had also suggested that
215 the effect of IL-18 differs depending on whether GVHD is mainly mediated by $CD8^+$ or
216 $CD4^+$ T cells in murine models(*42*). Our data suggest that, in humans, this effector phase
217 depends on the activation profile of $CD8^+$ T cells, and that IL-18 may worsen the severity of
218 CD8-mediated GVHD by increasing steroid resistance. IL18 is a proinflammatory cytokine
219 which can promote interferon γ production(*43*), and its serum level in post-HSCT patients was
220 associated with aGVHD severity ($r = 0.861$, $P < 0.001$)(*44*). Furthermore, our results highlight
221 the key role of TNFα production by myeloid cells in SR-GVHD on CD4+ T activation that could
222 amplify the alloimmune response. These results confirm data obtained in animal models and
223 show that myeloid subsets may not only participate in the initiation of GVHD(*19*) but that their
224 response profile could already initiate the first mechanisms of steroid resistance.

225 Interferon have been described for their crucial role in GVHD development(*45–47*). We
226 found that IFNα and γ pathways were enriched at time of aGVHD and before corticosteroid
227 treatment. However, SR-aGVHD was associated with lower activation of IFNα and γ pathways
228 in most immune subsets, except for naïve CD8 T cells and non-classical monocytes. This could
229 explain why in SR-aGVHD, INFG/IFNGR interactions increased cell-to-cell crosstalk between

230 CD8+ T cells, monocytes and CD4+ T cells. In addition, it has been suggested previously that
231 IFNγ production could contribute to increase the severity of digestive GVHD(*48*, *49*) and that
232 IFNλ blockade could improve gut GVHD severity(*50*).

233 Finally, trajectory inferences highlighted specific layouts associated with SR-aGVHD.
234 Cells were particularly abundant in low and high pseudotime in SR-GVHD patients, while there
235 was a progressive increase along pseudotime in SS-GVHD patients **(Figure 6)**. It suggests
236 that cells in SR-GVHD patients quickly differentiate to terminally activated states. This was
237 consistent with, higher and earlier gene expression of LAG3 and TIGIT in SR-GVHD patients.
238 Consistent with results from cell-cell interactions analysis, CCL4 and CCL5 were expressed at
239 higher levels and earlier in SR-GVHD patients, as also described in animal model(*51*).

240 Because samples were collected before cortico-steroid initiation, our work sheds light
241 on early signature pathways leading to steroid resistance. These pathways appeared distinct
242 from those involved in the general inflammatory response of acute GVHD and could be
243 targeted as early as steroid initiation. Transcriptomic analysis offered a powerful approach to
244 unravel immune cells functionality, combined with precise phenotypic population identification,
245 allowing for the identification of cellular heterogeneity in SR-GVHD immune response. The
246 complexity of the immune response in the context of GVHD was already investigated at the
247 single cell level, through T cell subset analysis following TCR clonotype mapping(*52*). This
248 elegant approach, revealed that each patient possessed a highly intricate repertoire, with
249 different tissues exhibiting distinct clonal populations, varying degrees of repertoire overlap
250 between sites, and diverse numbers of dominant clones shared across multiple tissues (*52*).
251 More recently, a similar approach highlighted the impact of the tissue microenvironment on
252 maintaining T-cell activation and driving divergent immune responses in peripheral organs
253 (*53*). Our results rely on PBMCs samples and hence, provide a complementary perspective on
254 acute GVHD, that uncover biological pathways associated with steroid resistance,
255 irrespectively of targeted organs. Studies based directly on blood samples are essential in

clinical practice, as they provide an easy access to potential predictors that could guide therapeutic management.

Our study offers new insights into the immune complexity, presenting a broader perspective of the immune response. Since our samples were all collected at onset of GVHD, the sampling time varied between patients, which could impact the immune response, particularly cytokine secretion. Therefore, while our study underscores the need for validation in a larger cohort with careful matching of sampling times, it could also serve as a robust basis for future studies involving a broader patient population. Furthermore, the use of models would require additional validation *in vivo*. Finally, additional studies focusing on immune infiltrates in target organs of GVHD would certainly help to complete our understanding of acute GVHD pathophysiology, and especially of mechanisms associated with corticosteroid resistance.

Overall, these findings provide evidence that corticosteroid resistance is an intrinsic mechanism already present at the onset of alloimmune response, highlighting specific patterns that may serve as potential new therapeutic targets.

272 # MATERIALS AND METHODS

273 **Cohort**

274 This study was conducted with annotated samples from patients and healthy donors provided
275 by the CRYOSTEM Consortium and the SFGM-TC (Société Francophone de Greffe de Moelle
276 et de Thérapie Cellulaire). Patients were included in the CRYOSTEM cohort after validation
277 by the scientific committee (study number CS 18-01). CRYOSTEM cohort and collection were
278 approved by IRB Sud-Méditerranée 1 (reference number DC-2014-2312 and DC-2019-3425)
279 and the Commission Nationale de l'Informatique et des Libertés for data protection (reference
280 number nz70243374i n°912120). All patients gave their written consent for clinical research
281 and sample collection. This non-interventional research study with no additional clinical
282 procedure was carried out in accordance with the Declaration of Helsinki. Data analyses were
283 carried out using an anonymized database. Healthy donor's PBMC were isolated from residual
284 blood after apheresis provided by Etablissement Français du Sang (18/EFS/032).
285

286 **CITE Seq experiment**

287 After thawing cells in a 50% fetal calf serum (FCS)/RPMI medium, 10x Genomics Feature
288 Barcoding recommendations were followed. Cells were washed twice using a 10 mL solution
289 of the same media. 500 000 cells were transferred in a 0.04% PBS/bovine serum albumin
290 (BSA) medium and washed. Cells were then suspended in a 1% PBS/BSA solution before
291 incubation with oligonucleotide-coupled antibodies TotalSeq-B (panel described in **Table S13**)
292 for 60 min on ice. Cells were washed 4 times (4°C, RCF 300, 5 minutes) and suspended to
293 obtain a concentration of 1 000 cells/µL. 10 000 cells were subjected in Gel Bead Emulsion
294 using Chromium 10x Genomics controller, according to manufacturer guidelines. Chromium™
295 Next GEM Single Cell 3' Kit v3.1 (10X Genomics, cat. 1000268) and 3' Feature Barcode Kit
296 (10X Genomics, cat. 1000262) were used to prepare reagents.

297 To perform single cell RNA sequencing after cDNA amplification, the concentration of
298 each sample was measured using Tapestation 2200 (Agilent). To prepare the cDNA libraries
299 for 10x Genomics Chromium controller, we used the single-cell 3′ v3.1 kit (Dual Index) with
300 Feature Barcode technology for Cell Surface Protein, following manufacturer guidelines. QC
301 libraries were performed using Tapestation 2200 (Agilent). Libraries were equimolar pooled to
302 obtain at least 20 000 read pairs per cell and 5 000 read pairs for feature barcode part after
303 sequencing on Illumina Novaseq 6000 (100 cycles cartridge). The input number of cells was
304 estimated at 10 000 cells/samples. FASTQ files were obtained with bcl2fastq (Illumina).
305

306 **Data quality control**

307 Alignment, filtering, barcode counting, UMI counting were performed with count function from
308 10x Genomics Cell Ranger (version 6.0) using GRCh38 genome assembly as reference data.
309 Then aggr function was used to aggregate results without normalization. A R environment
310 (version 4.3.1) was subsequently used for the following analyses. Briefly, using Seurat R
311 package(*54*), dead cells were excluded if mitochondrial RNA was above 18%; singlet were
312 identified as droplets with RNA feature between 200 and 4 700; RNA and cell surface antigen
313 counts were normalized and scaled using Seurat R package normalization and scaling function
314 for linear transformation. 2 000 highly variable RNA features were identified.
315

316 **Immune cell clustering**

317 Using a principal component analysis method on the scaled data, cells were clustered
318 according to cell surface antigen expression. We used UMAP for cluster visualization. Seurat
319 R package was then used to calculate cell cycle phase based on canonical transcripts, and
320 regressing these out of the data.
321

322 **Enrichment pathways analysis**

323 Fast pre-ranked gene set enrichment analysis was performed using FGSEA package(*55*) with
324 "hallmarks" gene reference data set from Molecular signature database(*56*). Pathways were
325 compared between GVHD and non-GVHD patients, and between SR-GVHD and SS-GVHD
326 patients. Gene expression comparison between GVHD and non GVHD patients, and between
327 SS- and SR-GVHD patients was provided by differential expression analysis. Enrichment
328 scores associated with adjusted p-value < 0.05 were selected for dot plot visualization.

329

330 **NicheNet Analysis**

331 Ligand-receptors interaction was computed using NicheNet package(*32*). Sender cells were
332 identified as myeloid cells, B cells, $CD4^+$ conventional T cells and regulatory T cells. Receiver
333 cells were identified as $CD4^+$ and $CD8^+$ T lymphocytes, NK cells and regulatory T cells. Three
334 pooled human gene expression data of interacting cells(*57–59*) were used as input and
335 combined with a prior model that integrates existing knowledge on ligand-to-target signaling
336 paths to perform ligand activity analyses. Circos plot visualization integrated *bona fide*
337 interactions of each receiver, and increased or decreased interactions were integrated from
338 "ligand differential expression heatmap" NicheNet output.

339

340 **Trajectory inferences**

341 Trajectory were based on RNA expression clustering (**Figure S10**). SingleCellExperiment
342 object was subset by immune populations (CD8+ T cells, CD4+ T cells, NK cells, B cells and
343 myeloid cells) before pseudotime calculation using slingshot package(*60*). TradSeq package
344 was then use for downstream analysis(*61*). Briefly, associationTest R function evidenced
345 genes whose expression is associated with pseudotime. Since pseudotime is a continuous
346 value, it was divided into 50 categories for graphical representation with heatmap. Only the
347 500 most expressed gene in SS- and SR-GVHD were selected for heatmap visualization

348 (**Table S3-S6**). Each point on X axis corresponded to a cell cluster with similar pseudotimes.
349 The immune populations represented on top of the heatmap corresponded to the immune cell
350 population most abundantly represented within the cell cluster (**Table S7-S10**). Gene markers
351 specific to low pseudotime or high pseudotime were found thanks to starVsEndTest command.
352 Expression along pseudotime in each condition was plotted for four genes from the top 100
353 starVsEndTest output **(Figure 5, Tables S11 and S12)**. To explore the pathways associated
354 with gene expression of the top 500 most expressed genes along pseudotime from each of
355 the 5 modules of the heatmap, we used over-representation analysis using enrichGO
356 command from clusterProfiler R package(*62*). Only pathways associated with adjusted
357 pval < 0.05 from "molecular functions" and "biological process" of the Gene Ontology
358 knowledgbase(*63*, *64*) were selected for dot plots visualization.
359

360 **List of Supplementary Materials**

361 **Figure S1 to S15**

362 Fig. S1: Immune populations in each group of patients

363 Fig. S2: Immunotype survival analysis

364 Fig. S3: Immunotype and clinical variables

365 Fig. S4: Immune cell abundance in SS- and SR-GVHD patients

366 Fig. S5: Cell cycle in SS- and SR-GVHD patients and enrichment pathways in aGVHD

367 Fig. S6: Pathway enrichments in aGVHD patients

368 Fig. S7: Interactions combined plots in regulatory T cells and NK cells

369 Fig. S8: Interactions combined plots in $CD4^+$ T cells and double negative T cells

370 Fig. S9: Bona fide interactions in all receivers

371 Fig. S10: Clustering based on RNA expression

372 Fig. S11: $CD8^+$ T cells lineage 2 trajectory analysis

373 Fig. S12: Over representation analysis in lineage 1 SR-GVHD patients

374 Fig. S13: Over representation analysis in lineage 1 SS-GVHD patients

375 Fig. S14: Over representation analysis in lineage 2 SR-GVHD patients

376 Fig. S15: Over representation analysis in lineage 2 SS-GVHD patients

377

378 **Table S1 to S2**

379 Table S1: Patients' characteristics

380 Table S2: Characteristics according to immunotypes

381

382 **Supplementary data files S3 to S13**

383 Data file S3: Top 500 genes expression matrix in lineage 1 SR-GVHD patients

384 Data file S4: Top 500 genes expression matrix in lineage 1 SS-GVHD patients

385 Data file S5: Top 500 genes expression matrix in lineage 2 SR-GVHD patients

386 Data file S6: Top 500 genes expression matrix in lineage 2 SS-GVHD patients

Data file S7: Immune population mostly represented along pseudotimes in lineage 1 SR-GVHD patients

Data file S8: Immune population mostly represented along pseudotimes in lineage 1 SS-GVHD patients

Data file S9: Immune population mostly represented along pseudotimes in lineage 1

2 SR-GVHD patients

Data file S10: Immune population mostly represented along pseudotimes in lineage 2 SS-GVHD patients

Data file S11: StartvsEnd output in lineage 1

Data file S12: StartvsEnd output in lineage 2

Data file S13: Total-Seq-B antibody panel

399 **REFERENCES**

400 1. N. Cieri, N. Hookeri, K. Stromhaug, L. Li, J. Keating, P. Díaz-Fernández, V. Gómez-García de
401 Soria, J. Stevens, R. Kfuri-Rubens, Y. Shao, K. A. Kooshesh, K. Powell, H. Ji, G. M. Hernandez, J.
402 Abelin, S. Klaeger, C. Forman, K. R. Clauser, S. Sarkizova, D. A. Braun, L. Penter, H. T. Kim, W. J.
403 Lane, G. Oliveira, L. S. Kean, S. Li, K. J. Livak, S. A. Carr, D. B. Keskin, C. Muñoz-Calleja, V. T. Ho,
404 J. Ritz, R. J. Soiffer, D. Neuberg, C. Stewart, G. Getz, C. J. Wu, Systematic identification of minor
405 histocompatibility antigens predicts outcomes of allogeneic hematopoietic cell transplantation. *Nat*
406 *Biotechnol*, 1–12 (2024).
407 2. R. Zeiser, B. R. Blazar, Acute Graft-versus-Host Disease — Biologic Process, Prevention, and
408 Therapy. *N Engl J Med* **377**, 2167–2179 (2017).
409 3. A. C. Harris, R. Young, S. Devine, W. J. Hogan, F. Ayuk, U. Bunworasate, C.
410 Chanswangphuwana, Y. A. Efebera, E. Holler, M. Litzow, R. Ordemann, M. Qayed, A. S. Renteria, R.
411 Reshef, M. Wölfl, Y.-B. Chen, S. Goldstein, M. Jagasia, F. Locatelli, S. Mielke, D. Porter, T. Schechter,
412 Z. Shekhovtsova, J. L. M. Ferrara, J. E. Levine, International, Multicenter Standardization of Acute
413 Graft-versus-Host Disease Clinical Data Collection: A Report from the Mount Sinai Acute GVHD
414 International Consortium. *Biol Blood Marrow Transplant* **22**, 4–10 (2016).
415 4. L. Axt, A. Naumann, J. Toennies, S. P. Haen, W. Vogel, D. Schneidawind, S. Wirths, R.
416 Moehle, C. Faul, L. Kanz, S. Axt, W. A. Bethge, Retrospective single center analysis of outcome, risk
417 factors and therapy in steroid refractory graft-versus-host disease after allogeneic hematopoietic cell
418 transplantation. *Bone Marrow Transplant* **54**, 1805–1814 (2019).
419 5. P. J. Martin, J. D. Rizzo, J. R. Wingard, K. Ballen, P. T. Curtin, C. Cutler, M. R. Litzow, Y.
420 Nieto, B. N. Savani, J. R. Schriber, P. J. Shaughnessy, D. A. Wall, P. A. Carpenter, First- and second-
421 line systemic treatment of acute graft-versus-host disease: recommendations of the American Society
422 of Blood and Marrow Transplantation. *Biol Blood Marrow Transplant* **18**, 1150–1163 (2012).
423 6. J. R. Westin, R. M. Saliba, M. De Lima, A. Alousi, C. Hosing, M. H. Qazilbash, I. F. Khouri,
424 E. J. Shpall, P. Anderlini, G. Rondon, B. S. Andersson, R. Champlin, D. R. Couriel, Steroid-Refractory
425 Acute GVHD: Predictors and Outcomes. *Adv Hematol* **2011**, 601953 (2011).
426 7. R. Zeiser, N. von Bubnoff, J. Butler, M. Mohty, D. Niederwieser, R. Or, J. Szer, E. M. Wagner,
427 T. Zuckerman, B. Mahuzier, J. Xu, C. Wilke, K. K. Gandhi, G. Socié, REACH2 Trial Group, Ruxolitinib
428 for Glucocorticoid-Refractory Acute Graft-versus-Host Disease. *N Engl J Med* **382**, 1800–1810 (2020).
429 8. O. Penack, M. Marchetti, M. Aljurf, M. Arat, F. Bonifazi, R. F. Duarte, S. Giebel, H. Greinix,
430 M. D. Hazenberg, N. Kröger, S. Mielke, M. Mohty, A. Nagler, J. Passweg, F. Patriarca, T. Ruutu, H.
431 Schoemans, C. Solano, R. Vrhovac, D. Wolff, R. Zeiser, A. Sureda, Z. Peric, Prophylaxis and
432 management of graft-versus-host disease after stem-cell transplantation for haematological
433 malignancies: updated consensus recommendations of the European Society for Blood and Marrow
434 Transplantation. *Lancet Haematol* **11**, e147–e159 (2024).
435 9. P. J. Martin, G. Schoch, L. Fisher, V. Byers, C. Anasetti, F. R. Appelbaum, P. G. Beatty, K.
436 Doney, G. B. McDonald, J. E. Sanders, A retrospective analysis of therapy for acute graft-versus-host
437 disease: initial treatment. *Blood* **76**, 1464–1472 (1990).
438 10. J. L. M. Ferrara, A. C. Harris, J. K. Greenson, T. M. Braun, E. Holler, T. Teshima, J. E. Levine,
439 S. W. J. Choi, E. Huber, K. Landfried, K. Akashi, M. Vander Lugt, P. Reddy, A. Chin, Q. Zhang, S.
440 Hanash, S. Paczesny, Regenerating islet-derived 3-alpha is a biomarker of gastrointestinal graft-versus-
441 host disease. *Blood* **118**, 6702–6708 (2011).
442 11. M. T. Vander Lugt, T. M. Braun, S. Hanash, J. Ritz, V. T. Ho, J. H. Antin, Q. Zhang, C.-H.
443 Wong, H. Wang, A. Chin, A. Gomez, A. C. Harris, J. E. Levine, S. W. Choi, D. Couriel, P. Reddy, J. L.
444 M. Ferrara, S. Paczesny, ST2 as a marker for risk of therapy-resistant graft-versus-host disease and
445 death. *N Engl J Med* **369**, 529–539 (2013).
446 12. M. J. Hartwell, U. Özbek, E. Holler, A. S. Renteria, H. Major-Monfried, P. Reddy, M. Aziz, W.
447 J. Hogan, F. Ayuk, Y. A. Efebera, E. O. Hexner, U. Bunworasate, M. Qayed, R. Ordemann, M. Wölfl,
448 S. Mielke, A. Pawarode, Y.-B. Chen, S. Devine, A. C. Harris, M. Jagasia, C. L. Kitko, M. R. Litzow,
449 N. Kröger, F. Locatelli, G. Morales, R. Nakamura, R. Reshef, W. Rösler, D. Weber, K. Wudhikarn, G.
450 A. Yanik, J. E. Levine, J. L. Ferrara, An early-biomarker algorithm predicts lethal graft-versus-host

disease and survival. *JCI Insight* **2**, e89798 (2017).
13. H. Major-Monfried, A. S. Renteria, A. Pawarode, P. Reddy, F. Ayuk, E. Holler, Y. A. Efebera, W. J. Hogan, M. Wölfl, M. Qayed, E. O. Hexner, K. Wudhikarn, R. Ordemann, R. Young, J. Shah, M. J. Hartwell, M. S. Chaudhry, M. Aziz, A. Etra, G. A. Yanik, N. Kröger, D. Weber, Y.-B. Chen, R. Nakamura, W. Rösler, C. L. Kitko, A. C. Harris, M. Pulsipher, R. Reshef, S. Kowalyk, G. Morales, I. Torres, U. Özbek, J. L. M. Ferrara, J. E. Levine, MAGIC biomarkers predict long-term outcomes for steroid-resistant acute GVHD. *Blood* **131**, 2846–2855 (2018).
14. G. Socié, D. Niederwieser, N. von Bubnoff, M. Mohty, J. Szer, R. Or, J. Garrett, A. Prahallad, C. Wilke, R. Zeiser, Prognostic value of blood biomarkers in steroid-refractory or steroid-dependent acute graft-versus-host disease: a REACH2 analysis. *Blood* **141**, 2771–2779 (2023).
15. Q. Song, X. Wang, X. Wu, T. H. Kang, H. Qin, D. Zhao, R. R. Jenq, M. R. M. van den Brink, A. D. Riggs, P. J. Martin, Y.-Z. Chen, D. Zeng, IL-22-dependent dysbiosis and mononuclear phagocyte depletion contribute to steroid-resistant gut graft-versus-host disease in mice. *Nat Commun* **12**, 805 (2021).
16. V. Arnhold, W. Y. Chang, S. A. Jansen, G. Thangavelu, M. Calafiore, P. Vinci, Y.-Y. Fu, T. Ito, S. Takashima, A. Egorova, J. Kuttiyara, A. Perlstein, M. van Hoesel, C. Liu, B. R. Blazar, C. A. Lindemans, A. M. Hanash, Corticosteroids impair epithelial regeneration in immune-mediated intestinal damage. *J Clin Invest* **134**, e155880 (2024).
17. T. Toubai, C. Rossi, I. Tawara, C. Liu, C. Zajac, K. Oravecz-Wilson, D. Peltier, Y. Sun, H. Fujiwara, S.-R. Wu, M. Riwes, I. Henig, S. Kim, P. Reddy, Murine Models of Steroid Refractory Graft-versus-Host Disease. *Sci Rep* **8**, 12475 (2018).
18. S. G. Holtan, A. Shabaneh, B. C. Betts, A. Rashidi, M. L. MacMillan, C. Ustun, K. Amin, B. P. Vaughn, J. Howard, A. Khoruts, M. Arora, T. E. DeFor, D. Johnson, B. R. Blazar, D. J. Weisdorf, J. Wang, Stress responses, M2 macrophages, and a distinct microbial signature in fatal intestinal acute graft-versus-host disease. *JCI Insight* **5**, e129762, 129762 (2019).
19. L. Schwab, L. Goroncy, S. Palaniyandi, S. Gautam, A. Triantafyllopoulou, A. Mocsai, W. Reichardt, F. J. Karlsson, S. V. Radhakrishnan, K. Hanke, A. Schmitt-Graeff, M. Freudenberg, F. D. von Loewenich, P. Wolf, F. Leonhardt, N. Baxan, D. Pfeifer, O. Schmah, A. Schönle, S. F. Martin, R. Mertelsmann, J. Duyster, J. Finke, M. Prinz, P. Henneke, H. Häcker, G. C. Hildebrandt, G. Häcker, R. Zeiser, Neutrophil granulocytes recruited upon translocation of intestinal bacteria enhance graft-versus-host disease via tissue damage. *Nat Med* **20**, 648–654 (2014).
20. J. Hülsdünker, K. J. Ottmüller, H. P. Neeff, M. Koyama, Z. Gao, O. S. Thomas, M. Follo, A. Al-Ahmad, G. Prinz, S. Duquesne, H. Dierbach, S. Kirschnek, T. Lämmermann, M. J. Blaser, B. T. Fife, B. R. Blazar, A. Beilhack, G. R. Hill, G. Häcker, R. Zeiser, Neutrophils provide cellular communication between ileum and mesenteric lymph nodes at graft-versus-host disease onset. *Blood* **131**, 1858–1869 (2018).
21. M. Pelletier, L. Maggi, A. Micheletti, E. Lazzeri, N. Tamassia, C. Costantini, L. Cosmi, C. Lunardi, F. Annunziato, S. Romagnani, M. A. Cassatella, Evidence for a cross-talk between human neutrophils and Th17 cells. *Blood* **115**, 335–343 (2010).
22. D. Minns, K. J. Smith, V. Alessandrini, G. Hardisty, L. Melrose, L. Jackson-Jones, A. S. MacDonald, D. J. Davidson, E. Gwyer Findlay, The neutrophil antimicrobial peptide cathelicidin promotes Th17 differentiation. *Nat Commun* **12**, 1285 (2021).
23. Q. Song, U. Nasri, D. Zeng, Steroid-Refractory Gut Graft-Versus-Host Disease: What We Have Learned From Basic Immunology and Experimental Mouse Model. *Front Immunol* **13**, 844271 (2022).
24. B. K. Patel, M. J. Raabe, E. R. Lang, Y. Song, C. Lu, V. Deshpande, L. T. Nieman, M. J. Aryee, Y.-B. Chen, D. T. Ting, Z. DeFilipp, Spatial transcriptomics reveals distinct tissue niches linked with steroid responsiveness in acute gastrointestinal GVHD. *Blood* **142**, 1831–1844 (2023).
25. R. R. Jenq, Y. Taur, S. M. Devlin, D. M. Ponce, J. D. Goldberg, K. F. Ahr, E. R. Littmann, L. Ling, A. C. Gobourne, L. C. Miller, M. D. Docampo, J. U. Peled, N. Arpaia, J. R. Cross, T. K. Peets, M. A. Lumish, Y. Shono, J. A. Dudakov, H. Poeck, A. M. Hanash, J. N. Barker, M.-A. Perales, S. A. Giralt, E. G. Pamer, M. R. M. van den Brink, Intestinal Blautia Is Associated with Reduced Death from Graft-versus-Host Disease. *Biol Blood Marrow Transplant* **21**, 1373–1383 (2015).
26. Y. Furusawa, Y. Obata, S. Fukuda, T. A. Endo, G. Nakato, D. Takahashi, Y. Nakanishi, C. Uetake, K. Kato, T. Kato, M. Takahashi, N. N. Fukuda, S. Murakami, E. Miyauchi, S. Hino, K. Atarashi,

S. Onawa, Y. Fujimura, T. Lockett, J. M. Clarke, D. L. Topping, M. Tomita, S. Hori, O. Ohara, T. Morita, H. Koseki, J. Kikuchi, K. Honda, K. Hase, H. Ohno, Commensal microbe-derived butyrate induces the differentiation of colonic regulatory T cells. *Nature* **504**, 446–450 (2013).

27. N. D. Mathewson, R. Jenq, A. V. Mathew, M. Koenigsknecht, A. Hanash, T. Toubai, K. Oravecz-Wilson, S.-R. Wu, Y. Sun, C. Rossi, H. Fujiwara, J. Byun, Y. Shono, C. Lindemans, M. Calafiore, T. M. Schmidt, K. Honda, V. B. Young, S. Pennathur, M. van den Brink, P. Reddy, Gut microbiome-derived metabolites modulate intestinal epithelial cell damage and mitigate graft-versus-host disease. *Nat Immunol* **17**, 505–513 (2016).

28. J. L. Golob, M. M. DeMeules, T. Loeffelholz, Z. Z. Quinn, M. K. Dame, S. S. Silvestri, M. C. Wu, T. M. Schmidt, T. L. Fiedler, M. J. Hoostal, M. Mielcarek, J. Spence, S. A. Pergam, D. N. Fredricks, Butyrogenic bacteria after acute graft-versus-host disease (GVHD) are associated with the development of steroid-refractory GVHD. *Blood Adv* **3**, 2866–2869 (2019).

29. M. Couturier, B. Lamarthée, J. Arbez, J.-C. Renauld, C. Bossard, F. Malard, F. Bonnefoy, M. Mohty, S. Perruche, P. Tiberghien, P. Saas, B. Gaugler, IL-22 deficiency in donor T cells attenuates murine acute graft-versus-host disease mortality while sparing the graft-versus-leukemia effect. *Leukemia* **27**, 1527–1537 (2013).

30. B. Lamarthée, F. Malard, C. Gamonet, C. Bossard, M. Couturier, J.-C. Renauld, M. Mohty, P. Saas, B. Gaugler, Donor interleukin-22 and host type I interferon signaling pathway participate in intestinal graft-versus-host disease via STAT1 activation and CXCL10. *Mucosal Immunol* **9**, 309–321 (2016).

31. M. A. Schroeder, J. F. DiPersio, Mouse models of graft-versus-host disease: advances and limitations. *Disease Models & Mechanisms* **4**, 318–333 (2011).

32. R. Browaeys, W. Saelens, Y. Saeys, NicheNet: modeling intercellular communication by linking ligands to target genes. *Nat Methods* **17**, 159–162 (2020).

33. D. R. Edwards, M. M. Handsley, C. J. Pennington, The ADAM metalloproteinases. *Mol Aspects Med* **29**, 258–289 (2008).

34. J. C. Albring, M. M. Sandau, A. S. Rapaport, B. T. Edelson, A. Satpathy, M. Mashayekhi, S. K. Lathrop, C.-S. Hsieh, M. Stelljes, M. Colonna, T. L. Murphy, K. M. Murphy, Targeting of B and T lymphocyte associated (BTLA) prevents graft-versus-host disease without global immunosuppression. *J Exp Med* **207**, 2551–2559 (2010).

35. Y. Sakoda, J.-J. Park, Y. Zhao, A. Kuramasu, D. Geng, Y. Liu, E. Davila, K. Tamada, Dichotomous regulation of GVHD through bidirectional functions of the BTLA-HVEM pathway. *Blood* **117**, 2506–2514 (2011).

36. F. Martins, E. Planet, D. Marino, M. Ansari, D. Trono, Single-cell transcriptome analysis reveals atypical monocytes circulating ahead of acute graft-versus-host disease clinical onset. *J Leukoc Biol*, qiae229 (2024).

37. H. Sun, L. Wu, X. Zhao, Y. Huo, P. Dong, A. Pang, Y. Zheng, Y. Han, S. Ma, E. Jiang, F. Dong, T. Cheng, S. Hao, Monocytes as an early risk factor for acute graft-versus-host disease after allogeneic hematopoietic stem cell transplantation. *Front Immunol* **15**, 1433091 (2024).

38. L. Jardine, U. Cytlak, M. Gunawan, G. Reynolds, K. Green, X.-N. Wang, S. Pagan, M. Paramitha, C. A. Lamb, A. K. Long, E. Hurst, S. Nair, G. H. Jackson, A. Publicover, V. Bigley, M. Haniffa, A. J. Simpson, M. Collin, Donor monocyte-derived macrophages promote human acute graft-versus-host disease. *J Clin Invest* **130**, 4574–4586 (2020).

39. K. Seno, M. Yasunaga, H. Kajiya, K. Izaki-Hagio, H. Morita, M. Yoneda, T. Hirofuji, J. Ohno, Dynamics of M1 macrophages in oral mucosal lesions during the development of acute graft-versus-host disease in rats. *Clin Exp Immunol* **190**, 315–327 (2017).

40. J. E. Levine, S. Paczesny, S. Mineishi, T. Braun, S. W. Choi, R. J. Hutchinson, D. Jones, Y. Khaled, C. L. Kitko, D. Bickley, O. Krijanovski, P. Reddy, G. Yanik, J. L. M. Ferrara, Etanercept plus methylprednisolone as initial therapy for acute graft-versus-host disease. *Blood* **111**, 2470–2475 (2008).

41. D. Jankovic, J. Ganesan, M. Bscheider, N. Stickel, F. C. Weber, G. Guarda, M. Follo, D. Pfeifer, A. Tardivel, K. Ludigs, A. Bouazzaoui, K. Kerl, J. C. Fischer, T. Haas, A. Schmitt-Gräff, A. Manoharan, L. Müller, J. Finke, S. F. Martin, O. Gorka, C. Peschel, J. Ruland, M. Idzko, J. Duyster, E. Holler, L. E. French, H. Poeck, E. Contassot, R. Zeiser, The Nlrp3 inflammasome regulates acute graft-versus-host disease. *J Exp Med* **210**, 1899–1910 (2013).

42. C.-K. Min, Y. Maeda, K. Lowler, C. Liu, S. Clouthier, D. Lofthus, E. Weisiger, J. L. M. Ferrara, P. Reddy, Paradoxical effects of interleukin-18 on the severity of acute graft-versus-host disease mediated by CD4+ and CD8+ T-cell subsets after experimental allogeneic bone marrow transplantation. *Blood* **104**, 3393–3399 (2004).
43. H. Okamura, H. Tsutsi, T. Komatsu, M. Yutsudo, A. Hakura, T. Tanimoto, K. Torigoe, T. Okura, Y. Nukada, K. Hattori, Cloning of a new cytokine that induces IFN-gamma production by T cells. *Nature* **378**, 88–91 (1995).
44. Y. Fujimori, H. Takatsuka, Y. Takemoto, H. Hara, H. Okamura, K. Nakanishi, E. Kakishita, Elevated interleukin (IL)-18 levels during acute graft-versus-host disease after allogeneic bone marrow transplantation. *Br J Haematol* **109**, 652–657 (2000).
45. R. J. Robb, G. R. Hill, The interferon-dependent orchestration of innate and adaptive immunity after transplantation. *Blood* **119**, 5351–5358 (2012).
46. S. Wang, T. Cheng, X. Chen, C. Zeng, W. Qin, Y. Xu, IFN-γ induces acute graft-versus-host disease by promoting HMGB1-mediated nuclear-to-cytoplasm translocation and autophagic degradation of p53. *Clin Sci (Lond)* **138**, 1287–1304 (2024).
47. F. T. Hakim, S. Memon, P. Jin, M. M. Imanguli, H. Wang, N. Rehman, X.-Y. Yan, J. Rose, J. W. Mays, S. Dhamala, V. Kapoor, W. Telford, J. Dickinson, S. Davis, D. Halverson, H. B. Naik, K. Baird, D. Fowler, D. Stroncek, E. W. Cowen, S. Z. Pavletic, R. E. Gress, Upregulation of IFN-Inducible and Damage-Response Pathways in Chronic Graft-versus-Host Disease. *J Immunol* **197**, 3490–3503 (2016).
48. T. Ara, D. Hashimoto, E. Hayase, C. Noizat, R. Kikuchi, Y. Hasegawa, K. Matsuda, S. Ono, Y. Matsuno, K. Ebata, R. Ogasawara, S. Takahashi, H. Ohigashi, E. Yokoyama, K. Matsuo, J. Sugita, M. Onozawa, R. Okumura, K. Takeda, T. Teshima, Intestinal goblet cells protect against GVHD after allogeneic stem cell transplantation via Lypd8. *Science Translational Medicine* **12**, eaaw0720 (2020).
49. Q. Song, U. Nasri, D. Zeng, Steroid-Refractory Gut Graft-Versus-Host Disease: What We Have Learned From Basic Immunology and Experimental Mouse Model. *Front. Immunol.* **13** (2022).
50. A. S. Henden, M. Koyama, R. J. Robb, A. Forero, R. D. Kuns, K. Chang, K. S. Ensbey, A. Varelias, S. H. Kazakoff, N. Waddell, A. D. Clouston, R. Giri, J. Begun, B. R. Blazar, M. A. Degli-Esposti, S. V. Kotenko, S. W. Lane, K. L. Bowerman, R. Savan, P. Hugenholtz, K. H. Gartlan, G. R. Hill, IFN-λ therapy prevents severe gastrointestinal graft-versus-host disease. *Blood* **138**, 722–737 (2021).
51. S. W. Choi, G. C. Hildebrandt, K. M. Olkiewicz, D. A. Hanauer, M. N. Chaudhary, I. A. Silva, C. E. Rogers, D. T. Deurloo, J. M. Fisher, C. Liu, D. Adams, S. W. Chensue, K. R. Cooke, CCR1/CCL5 (RANTES) receptor-ligand interactions modulate allogeneic T-cell responses and graft-versus-host disease following stem-cell transplantation. *Blood* **110**, 3447–3455 (2007).
52. S. DeWolf, Y. Elhanati, K. Nichols, N. R. Waters, C. L. Nguyen, J. B. Slingerland, N. Rodriguez, O. Lyudovyk, P. A. Giardina, A. I. Kousa, H. Andrlová, N. Ceglia, T. Fei, R. Kappagantula, Y. Li, N. Aleynick, P. Baez, R. Murali, A. Hayashi, N. Lee, B. Gipson, M. Rangesa, Z. Katsamakis, A. Dai, A. G. Blouin, M. Arcila, I. Masilionis, R. Chaligne, D. M. Ponce, H. J. Landau, I. Politikos, R. Tamari, A. M. Hanash, R. R. Jenq, S. A. Giralt, K. A. Markey, Y. Zhang, M.-A. Perales, N. D. Socci, B. D. Greenbaum, C. A. Iacobuzio-Donahue, T. J. Hollmann, M. R. M. van den Brink, J. U. Peled, Tissue-specific features of the T cell repertoire after allogeneic hematopoietic cell transplantation in human and mouse. *Sci Transl Med* **15**, eabq0476 (2023).
53. K. I. Omdahl, R. S. Bermea, R. Fleming, K. Kimler, J. Kaminski, L. P. Hariri, A. Ly, X. Rui, L. Cagnin, J. Lane, U. Gerdemann, B. R. Blazar, V. Tkachev, L. S. Kean, Organ-specific microenvironments drive divergent T cell evolution in acute graft-versus-host disease. *Sci Transl Med* **17**, eads1298 (2025).
54. Y. Hao, S. Hao, E. Andersen-Nissen, W. M. Mauck, S. Zheng, A. Butler, M. J. Lee, A. J. Wilk, C. Darby, M. Zager, P. Hoffman, M. Stoeckius, E. Papalexi, E. P. Mimitou, J. Jain, A. Srivastava, T. Stuart, L. M. Fleming, B. Yeung, A. J. Rogers, J. M. McElrath, C. A. Blish, R. Gottardo, P. Smibert, R. Satija, Integrated analysis of multimodal single-cell data. *Cell* **184**, 3573-3587.e29 (2021).
55. G. Korotkevich, V. Sukhov, N. Budin, B. Shpak, M. N. Artyomov, A. Sergushichev, Fast gene set enrichment analysis. bioRxiv [Preprint] (2021). https://doi.org/10.1101/060012.
56. A. Liberzon, C. Birger, H. Thorvaldsdóttir, M. Ghandi, J. P. Mesirov, P. Tamayo, The Molecular

Signatures Database (MSigDB) hallmark gene set collection. *Cell Syst* **1**, 417–425 (2015).
57. J. A. Ramilowski, T. Goldberg, J. Harshbarger, E. Kloppmann, M. Lizio, V. P. Satagopam, M. Itoh, H. Kawaji, P. Carninci, B. Rost, A. R. R. Forrest, A draft network of ligand-receptor-mediated multicellular signalling in human. *Nat Commun* **6**, 7866 (2015).
58. A. J. Pawson, J. L. Sharman, H. E. Benson, E. Faccenda, S. P. H. Alexander, O. P. Buneman, A. P. Davenport, J. C. McGrath, J. A. Peters, C. Southan, M. Spedding, W. Yu, A. J. Harmar, NC-IUPHAR, The IUPHAR/BPS Guide to PHARMACOLOGY: an expert-driven knowledgebase of drug targets and their ligands. *Nucleic Acids Res* **42**, D1098-1106 (2014).
59. A. D. Rouillard, G. W. Gundersen, N. F. Fernandez, Z. Wang, C. D. Monteiro, M. G. McDermott, A. Ma'ayan, The harmonizome: a collection of processed datasets gathered to serve and mine knowledge about genes and proteins. *Database (Oxford)* **2016**, baw100 (2016).
60. K. Street, D. Risso, R. B. Fletcher, D. Das, J. Ngai, N. Yosef, E. Purdom, S. Dudoit, Slingshot: cell lineage and pseudotime inference for single-cell transcriptomics. *BMC Genomics* **19**, 477 (2018).
61. K. Van den Berge, H. Roux de Bézieux, K. Street, W. Saelens, R. Cannoodt, Y. Saeys, S. Dudoit, L. Clement, Trajectory-based differential expression analysis for single-cell sequencing data. *Nat Commun* **11**, 1201 (2020).
62. G. Yu, L.-G. Wang, Y. Han, Q.-Y. He, clusterProfiler: an R package for comparing biological themes among gene clusters. *OMICS* **16**, 284–287 (2012).
63. M. Ashburner, C. A. Ball, J. A. Blake, D. Botstein, H. Butler, J. M. Cherry, A. P. Davis, K. Dolinski, S. S. Dwight, J. T. Eppig, M. A. Harris, D. P. Hill, L. Issel-Tarver, A. Kasarskis, S. Lewis, J. C. Matese, J. E. Richardson, M. Ringwald, G. M. Rubin, G. Sherlock, Gene Ontology: tool for the unification of biology. *Nat Genet* **25**, 25–29 (2000).
64. The Gene Ontology Consortium, S. A. Aleksander, J. Balhoff, S. Carbon, J. M. Cherry, H. J. Drabkin, D. Ebert, M. Feuermann, P. Gaudet, N. L. Harris, D. P. Hill, R. Lee, H. Mi, S. Moxon, C. J. Mungall, A. Muruganugan, T. Mushayahama, P. W. Sternberg, P. D. Thomas, K. Van Auken, J. Ramsey, D. A. Siegele, R. L. Chisholm, P. Fey, M. C. Aspromonte, M. V. Nugnes, F. Quaglia, S. Tosatto, M. Giglio, S. Nadendla, G. Antonazzo, H. Attrill, G. dos Santos, S. Marygold, V. Strelets, C. J. Tabone, J. Thurmond, P. Zhou, S. H. Ahmed, P. Asanitthong, D. Luna Buitrago, M. N. Erdol, M. C. Gage, M. Ali Kadhum, K. Y. C. Li, M. Long, A. Michalak, A. Pesala, A. Pritazahra, S. C. C. Saverimuttu, R. Su, K. E. Thurlow, R. C. Lovering, C. Logie, S. Oliferenko, J. Blake, K. Christie, L. Corbani, M. E. Dolan, H. J. Drabkin, D. P. Hill, L. Ni, D. Sitnikov, C. Smith, A. Cuzick, J. Seager, L. Cooper, J. Elser, P. Jaiswal, P. Gupta, P. Jaiswal, S. Naithani, M. Lera-Ramirez, K. Rutherford, V. Wood, J. L. De Pons, M. R. Dwinell, G. T. Hayman, M. L. Kaldunski, A. E. Kwitek, S. J. F. Laulederkind, M. A. Tutaj, M. Vedi, S.-J. Wang, P. D'Eustachio, L. Aimo, K. Axelsen, A. Bridge, N. Hyka-Nouspikel, A. Morgat, S. A. Aleksander, J. M. Cherry, S. R. Engel, K. Karra, S. R. Miyasato, R. S. Nash, M. S. Skrzypek, S. Weng, E. D. Wong, E. Bakker, T. Z. Berardini, L. Reiser, A. Auchincloss, K. Axelsen, G. Argoud-Puy, M.-C. Blatter, E. Boutet, L. Breuza, A. Bridge, C. Casals-Casas, E. Coudert, A. Estreicher, M. Livia Famiglietti, M. Feuermann, A. Gos, N. Gruaz-Gumowski, C. Hulo, N. Hyka-Nouspikel, F. Jungo, P. Le Mercier, D. Lieberherr, P. Masson, A. Morgat, I. Pedruzzi, L. Pourcel, S. Poux, C. Rivoire, S. Sundaram, A. Bateman, E. Bowler-Barnett, H. Bye-A-Jee, P. Denny, A. Ignatchenko, R. Ishtiaq, A. Lock, Y. Lussi, M. Magrane, M. J. Martin, S. Orchard, P. Raposo, E. Speretta, N. Tyagi, K. Warner, R. Zaru, A. D. Diehl, R. Lee, J. Chan, S. Diamantakis, D. Raciti, M. Zarowiecki, M. Fisher, C. James-Zorn, V. Ponferrada, A. Zorn, S. Ramachandran, L. Ruzicka, M. Westerfield, The Gene Ontology knowledgebase in 2023. *Genetics* **224**, iyad031 (2023).

Acknowledgments: The authors thank the patients who agreed to participate in this study by providing their blood samples. We also thank the iGenSeq platform team at ICM for sequencing the PBMC samples. We are grateful to the CRYOSTEM Consortium and the SFGM-TC for collecting patient samples and clinical data. **Funding:** This project was funded by la Fédération Leucémie Espoir and Fondation Maladies Rare (HPN-AM). **Author contributions:** Conceptualization: SLG, DM; Methodology: SLG, NV, DM; Samples processing: SLG, DB, YM, EB; Investigation: SLG, NV, DM; Visualization: SLG, GS, RPD, NV, DM; Funding acquisition: DM; Project administration: EB, DM, GS, RPD; Supervision: NV, DM; Writing – original draft: SLG, NV, DM; Draft revision: SLG, YM, DB, EB, RPF, GS, NV, DM. **Competing interests:** DM received research grants from Novartis and Sanofi, and consulting fees from Sanofi, Incyte, Novartis, Jazz Pharmaceuticals, CSL Behring and Mallinckrodt. Other authors declared that they have no competing interests. **Data availability:** Raw data are available on GEO public repository: GSE229733. Source code to reproduce the analyses, figures, and tables described in this manuscript are provided in a Git repository: https://gitlab.com/SophieLG/gvh_transcriptomic and long term preserved in Software Heritage:

https://archive.softwareheritage.org/browse/origin/directory/?origin_url=https://gitlab.com/SophieLG/gvh_transcriptomic&timestamp=2024-12-09T14:03:56.753000%2B00:00

677 **Figures legends:**

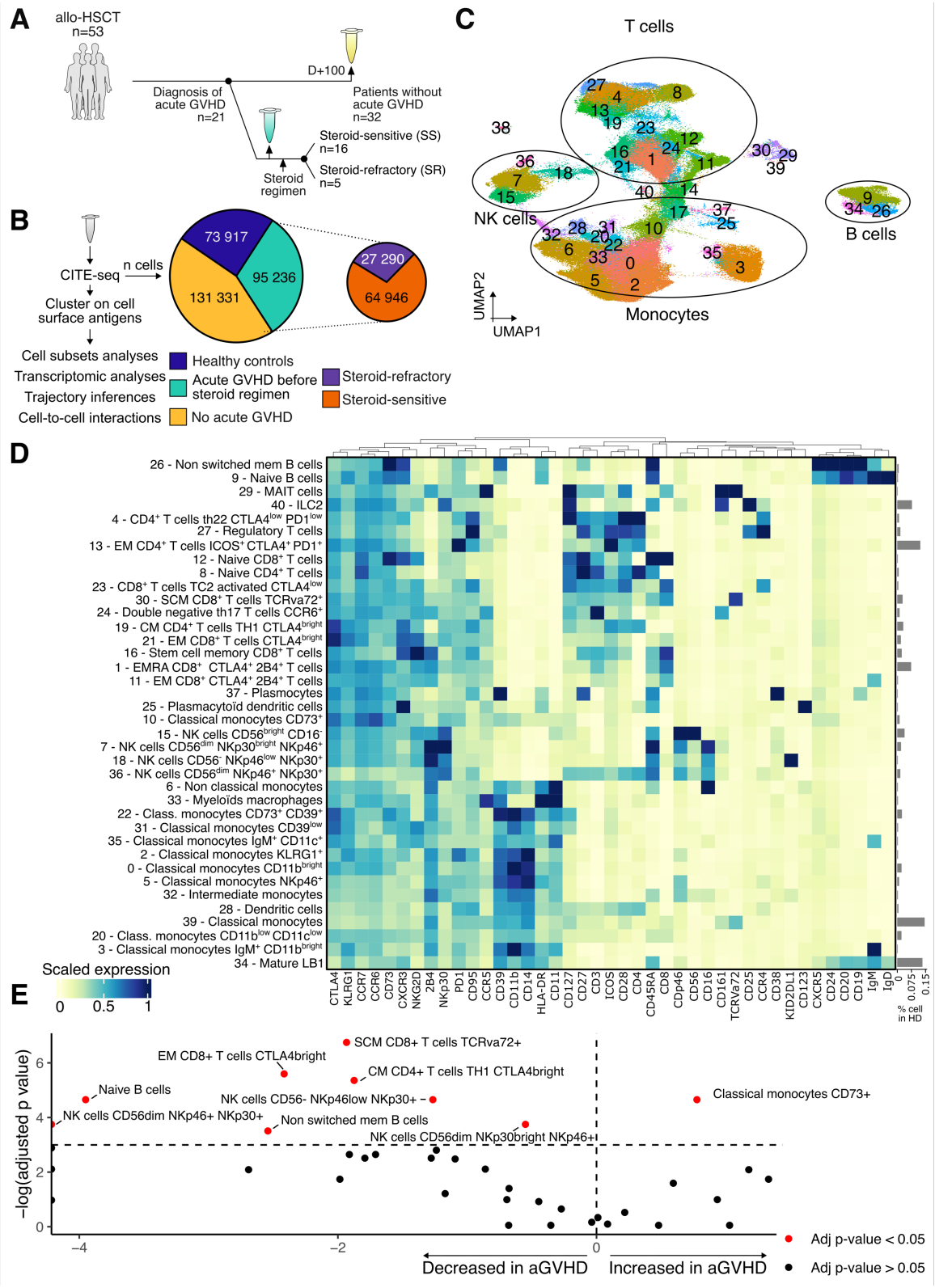

678

679 **Figure 1: Overview of patient and cell distribution, cluster identification, and relative**

680 **abundance of immune cell populations.**

681 **A:** Experimental design: HSCT patients (n=53) with (n=21) and without aGVHD (n=32) and
682 healthy donor as control group (n=6) were analyzed. PBMC were collected at day 100 post
683 HSCT for patients without aGVHD, and before steroid initiation for patients with aGVHD.
684 **B:** Number of cells included in the analysis after CITE-Seq processing. **C:** Uniform Manifold
685 Approximation and Projection (UMAP) after principal component analysis for immune cells
686 clustering, according to surface markers. **D:** Heatmap depicting immune cluster's identification
687 through surface antigen expression. Three irrelevant populations were removed and are
688 shown in **Figure S1**. **E**: Volcano plot exhibiting immune cells abundance in GVHD or
689 non-GVHD condition. Y axis reflects que -log 10(adjusted p-value) from differential expression
690 output, using non-parametric Mann-Whitney-Wilcoxon rank sum test. X axis reflects the
691 log(ratio) of median abundance in aGVHD condition, over non-aGVHD condition. Abbreviation:
692 CITE-Seq: Cellular indexing of transcriptomes and epitopes sequencing. aGVHD: acute graft
693 versus host disease. HSCT: allogeneic hematopoietic stem cell transplantation. PBMC:
694 Peripheral Blood Mononuclear Cells. SS-aGVHD: steroid sensitive acute graft versus host
695 disease. SR-aGVHD: steroid resistant acute graft versus host disease.

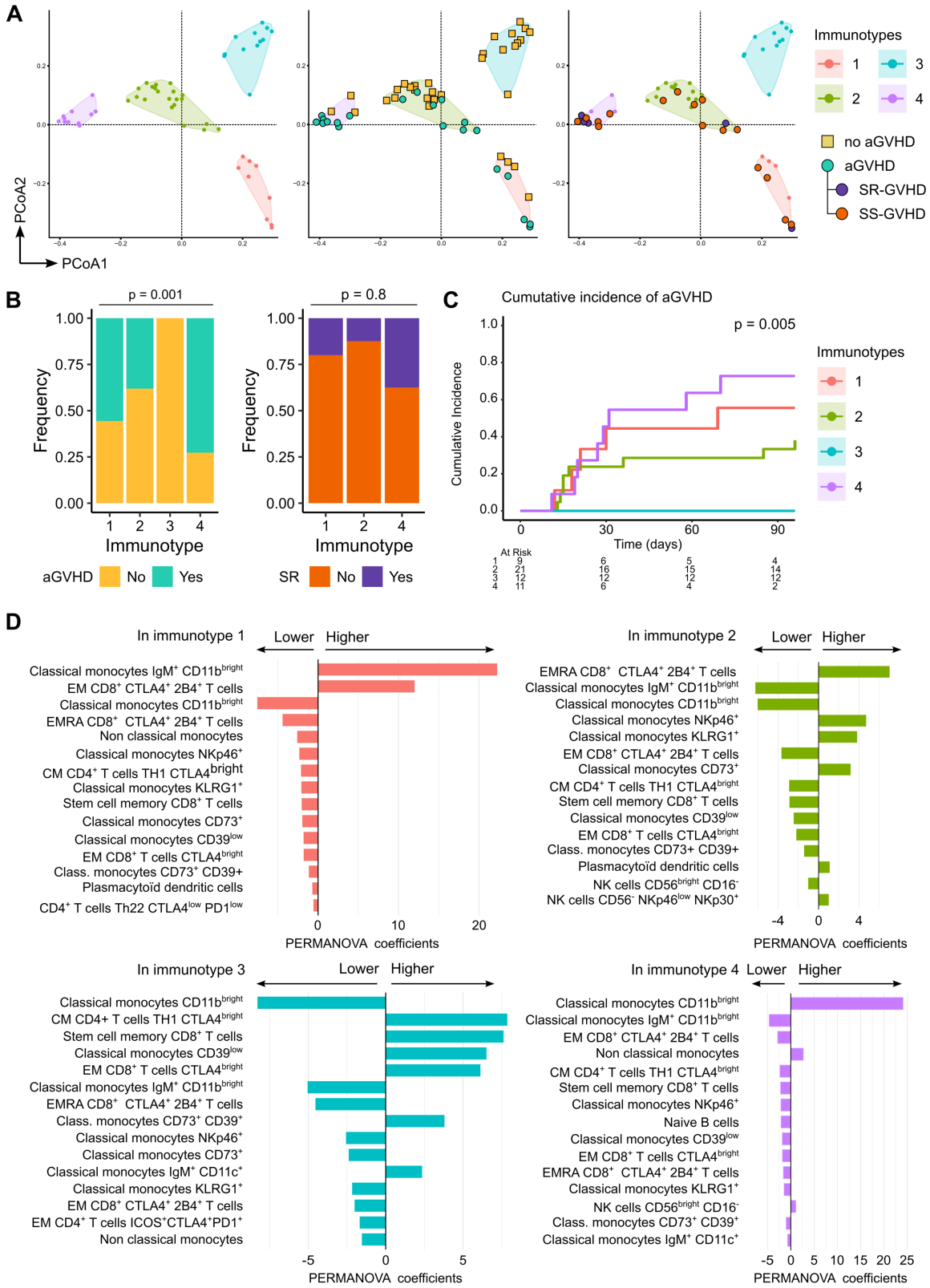

Figure 2: Immunotypes distinguished different immune patterns associated with aGVHD incidence.

699 **A:** Principal coordinates analysis (PCoA) revealed 4 different immune clusters (immunotypes)
700 according to cell population composition. **B:** Distribution of aGVHD patients among
701 immunotypes (left panel) and corticosteroid sensitivity (right panel). Fisher test was used for
702 statistical analysis. **C:** GVHD cumulative incidence with death as competing risk, estimated by
703 Kaplan-Meir method, Log rank test was used for statistical analysis. Immunotype 4 cumulative
704 incidence at day 100 = 72%, Immunotype 3 cumulative incidence at day 100 = 0%,
705 Immunotype 2 cumulative incidence at day 100 = 38%, Immunotype 1 cumulative incidence at
706 day 100 = 55%, log-rank p-value = 0.005. **D:** Bar plots showing top 15 contributing immune
707 subsets to immunotypes. Contribution was determined with permutational multivariate analysis
708 of variance (PERMANOVA).

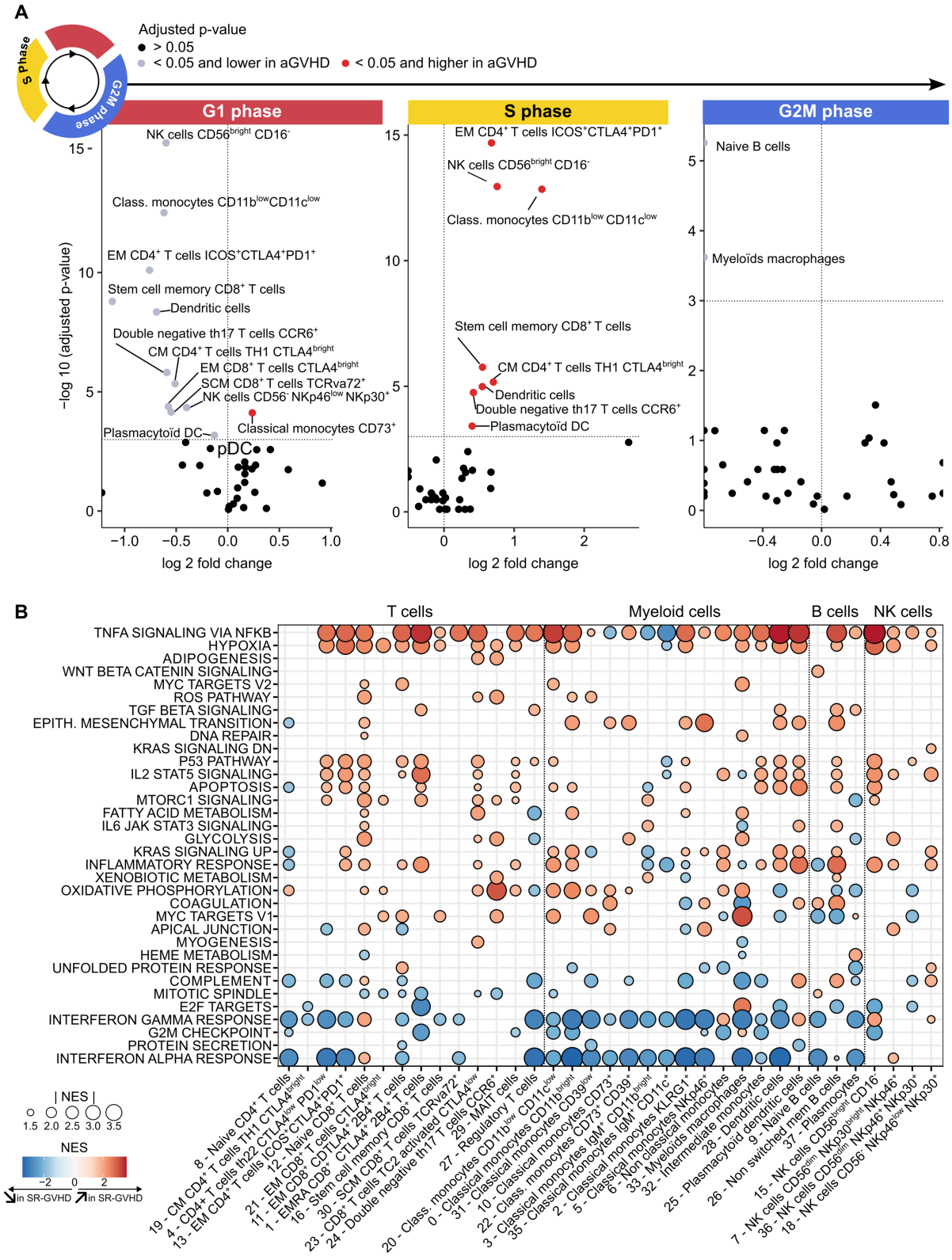

Figure 3: Cellular function analysis identified distinct features associated with SR-GVHD.

712 **A:** Volcano plots exhibiting cell cycle analysis after cell cycle phases scoring. X axis represents
713 log ratio of median number of cells in each phase in aGVHD patients over non GVHD patients.
714 Y axis represents log adjusted p values. Immune population significantly increased or
715 decreased are marked in red. Mann-Whitney-Wilcoxon tests were performed for statistical
716 analysis, and p values were adjusted using Benjamini and Hochberg method. **B:** Pathways
717 enrichment analysis comparing SR and SS-aGVHD, using gene set enrichment method and
718 "hallmarks" gene reference data set. Only significant values with adjusted p-value < 0.05 are
719 shown. NES: normalized enrichment score. SS-aGVHD: steroid sensitive acute graft versus
720 host disease. SR-aGVHD: steroid resistant acute graft versus host disease.

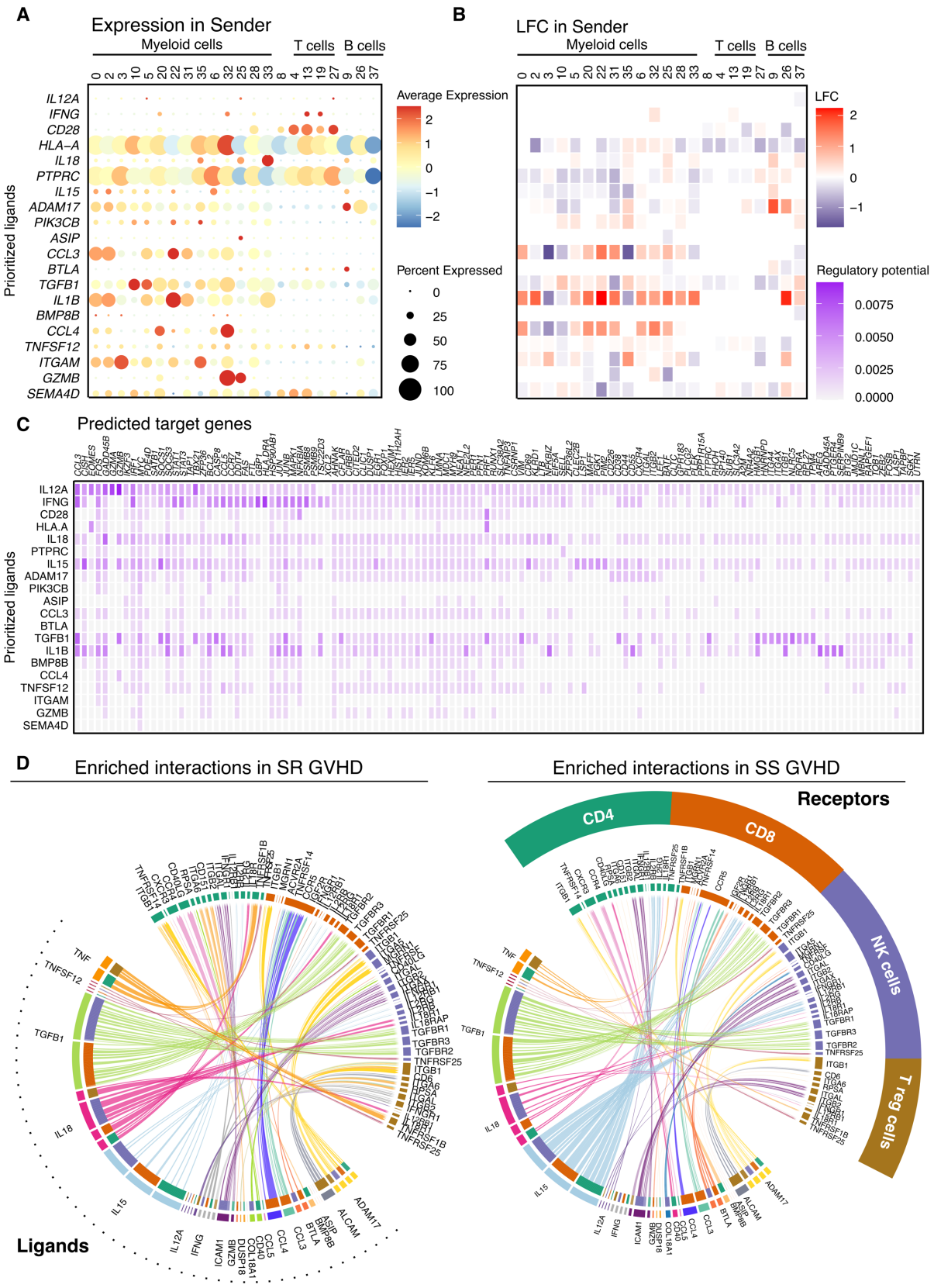

Figure 4: Cell-cell interactions with CD8+ T cells as receiver revealed specific patterns associated with SR-aGVHD

724 NicheNet Output when focusing on CD8+ T cells as receiver is depicted on panel A, B and C.
725 **A:** Expression of top-ranked ligands on sender cells. Prioritized ligands identified are exhibited
726 on Y axis, and sender cells on X axis. The color determines the average expression and the
727 point size the percent of senders expressing the ligand. **B:** Relative expression of ligands on
728 sender cells. Expression is exhibited in log fold change (red: increase expression in
729 SR-aGVHD patients, Blue: decreased expression in SR-aGVHD patients). **C:** Ligand–target
730 matrix exhibiting the regulatory potential of interactions. On the X axis is shown the active
731 targets genes of the top-ranked ligands. Heatmap visualization showing which top-ranked
732 ligands are predicted to have regulated the expression of which differentially expressed genes.
733 **D:** Circos plots depicting interactions between senders and all receiver cells. Ligands are
734 shown on the left side of the circos plot, and targets on the right side. Only *bona fide*
735 interactions were selected (**Figure S9A**). Links exhibits positive log fold change (left panel,
736 increased in SR-aGVHD patients) or negative log fold change (right panel, increased in
737 SS-aGVHD patients) from “ligand differential expression heatmap” NicheNet’s output. The
738 thickness of the link represents the numbers of sender populations involved in the interaction.
739 SR-aGVHD: Steroid resistant acute graft versus host disease. SS-aGVHD: Steroid sensitive
740 acute graft versus host disease.

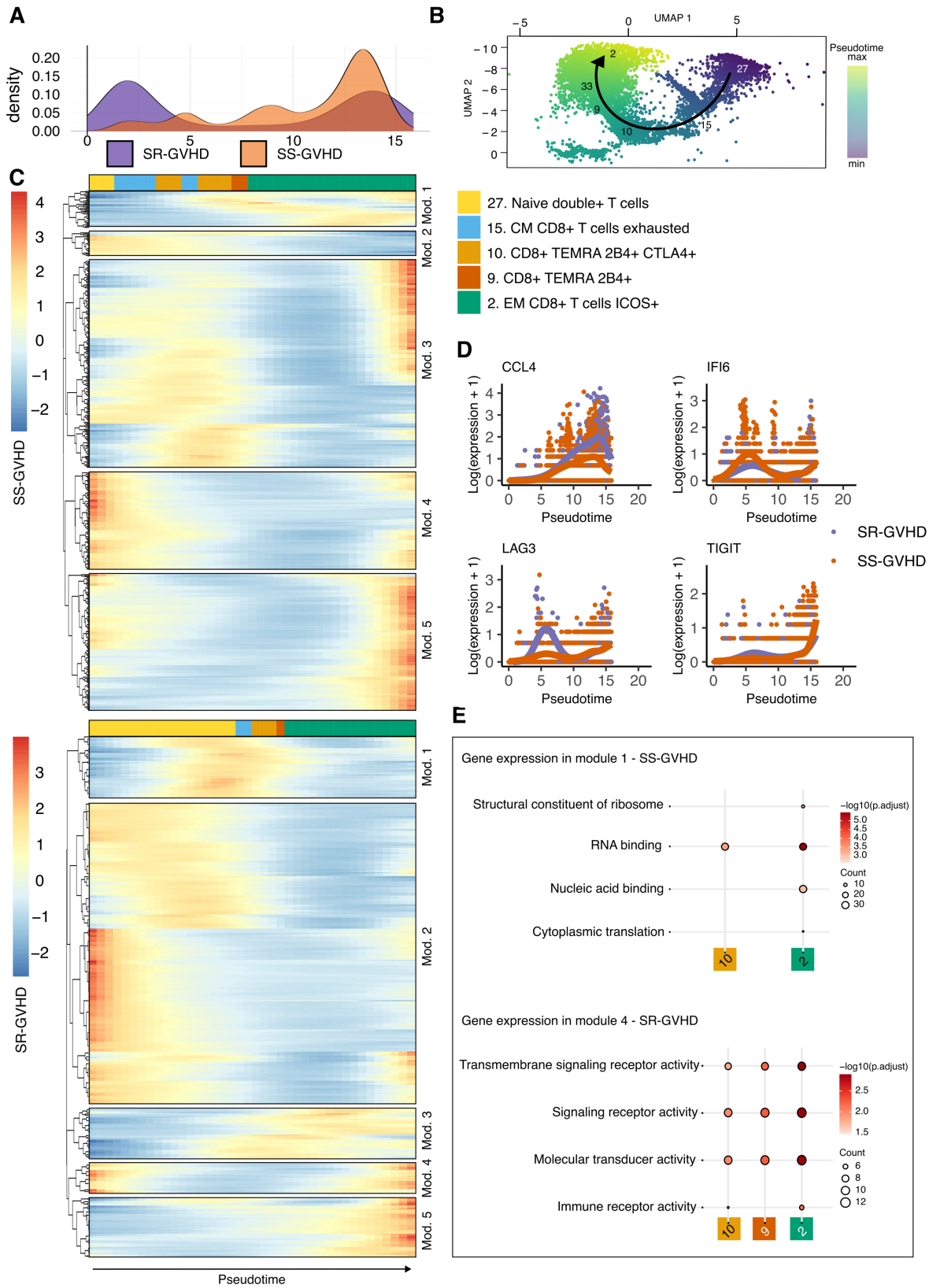

Figure 5: SR-aGVHD is associated with specific trajectory in CD8$^+$ T cells

743 **A:** Density plot for number of cells according to lineage 1 pseudotime visualization. SR-aGVHD
744 cell abundance was marked in low and high pseudotimes, while SS-aGVHD was associated
745 with a continuous increase in cell abundance along differentiation. **B:** Lineage 1 trajectory on
746 RNA clustering. **C:** Heatmap depicting gene expression among the top 500 most expressed
747 genes in SS-aGVHD patient (top panel) and in SR-aGVHD patients (low panel), along
748 pseudotime. The color at the top of each heatmap represents the immune population in which
749 the gene is expressed. **D:** Expression along pseudotime of four of the top 100 genes, whose
750 expression varied the most between the start and end points of a lineage.
751 **E:** Over-representation analysis to identify pathways associated with genes expression from
752 each module of the heatmaps. Only pathways associated with adjusted pval < 0.05 from
753 "molecular functions" and "biological process" of the Gene Ontology knowledgbase(*63*, *64*)
754 were selected for dot plots visualization. SR-aGVHD: Steroid resistant acute graft versus host
755 disease. SS-aGVHD: Steroid sensitive acute graft versus host disease.
756

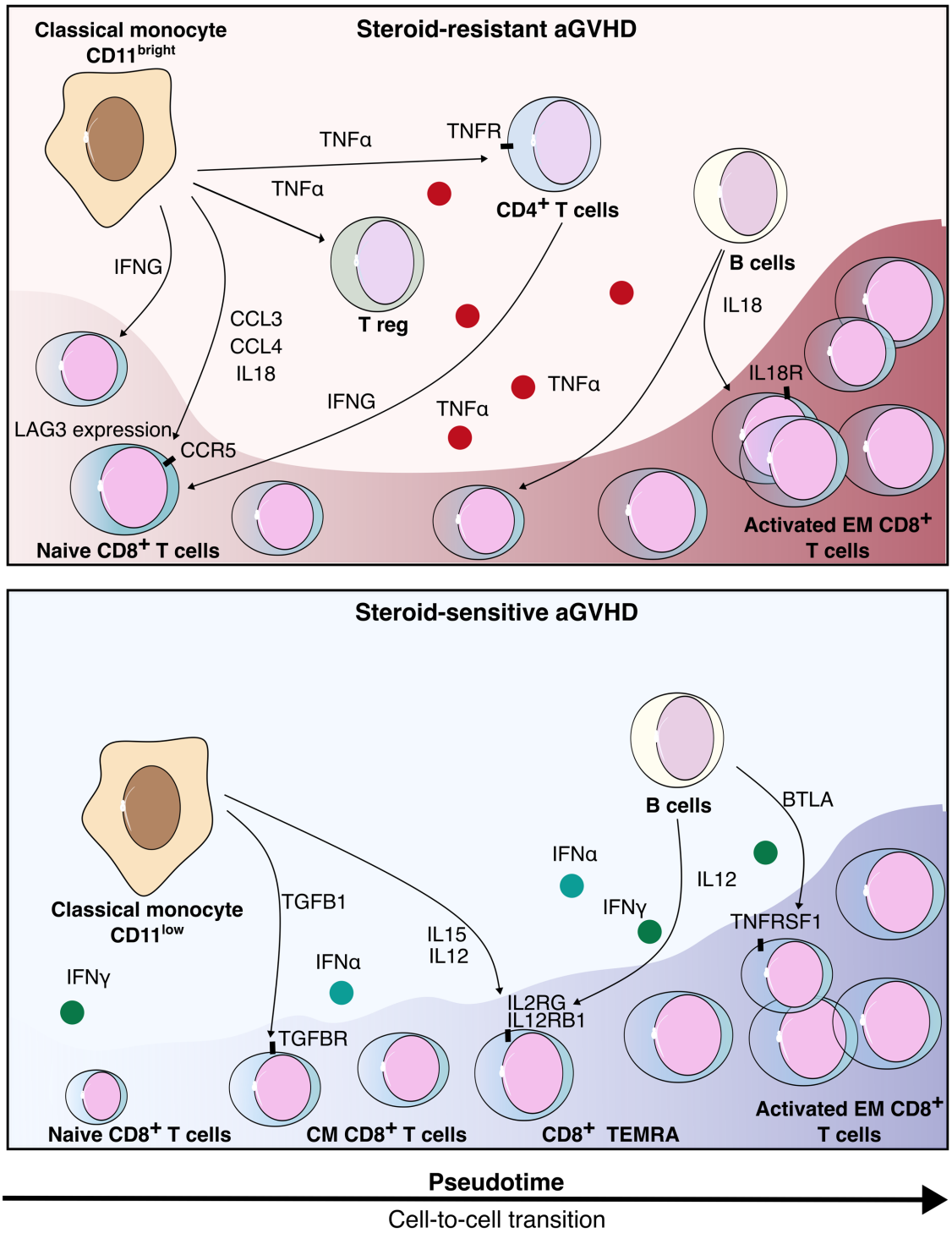

Figure 6: Steroid resistance is driven by biological pathways and specific networks of interaction

Steroid-resistant aGVHD results of cytokine production by myeloid populations, especially classical monocytes producing CCL3, CCL4, and IL18, which stimulate the activation of naive

762 $CD8^+$ T cells and induce direct differentiation into effector T cells. By contrast, steroid-sensitive
763 aGVHD is mainly driven by IL15 and IL12 production from classical monocytes and B cells,
764 and multiple transition states, from naïve $CD8^+$ T cells to activated EM $CD8^+$ T cells. aGVHD:
765 acute graft versus host disease, CM $CD8^+$ T cells: Central Memory $CD8^+$ T cells, EM $CD8^+$ T
766 cells: Effector Memory $CD8^+$ T cells, TEMRA $CD8^+$ T cells: Terminally differenciated Effector
767 Memory $CD8^+$ T cells